Analysis of Heavy Minerals Existence using Multispectral Satellite Imagery in Teknaf Upazila of Bangladesh

Farhana Tazneen[1*], A. Z. Md. Zahedul Islam[1], Md. Abdus Salam[1], Mohammad Rajib[2], Md. Masud Karim[3], and Md. Fahad Hossain[3]

[1]Bangladesh Space Research and Remote Sensing Organization (SPARRSO), Agargaon, Sher-e-Bangla Nagar, Dhaka-1207, Bangladesh

[2] Institute of Nuclear Minerals, Atomic Energy Research Establishment, Bangladesh Atomic Energy Commission, Ganakbari, Savar, Dhaka-1349

[3] Beach Sand Minerals Exploitation Center, Bangladesh Atomic Energy Commission

**Corresponding Author: E-mail: farhana@sparrso.gov.bd, nishigeoju@yahoo.com*

Abstract

In geological exploration optical remote sensing data has been an important tool for certain deposit types. Mineral resources are one of the important factors in the plans and programs of any country's economic development. The Teknaf coast of Cox's Bazar district is rich in minerals. For identifying heavy minerals in this area standardized hyperspectral analysis has been carried out using Landsat satellite data and Environment for Visualizing Images (ENVI) software. By comparing the spectral signatures with predefined spectral plots from the United States Geological Survey (USGS) spectral library selected endmembers are identified. Lastly, the endmembers are mapped with ENVI's spectral angle mapper (SAM). The minerals which show significant variation in reflectance at different spectral bands can be effectively mapped by using multispectral data. The classified image shows that a large amount of augite, ilmenite, garnet, rutile, and zircon are deposited along the shoreline of the study area. Field verifications are performed to assess the presence of minerals. The area is dominated by garnet, ilmenite & magnetite with considerable amount of zircon, rutile, and monazite. Heavy minerals concentration is relatively greater in subsurface. The presence of these minerals may vary from time to time due to humidity conditions, vegetation cover and atmospheric influences. Use of high spatial, hyperspectral satellite image can be enhanced for precision of analysis.

Keywords: Heavy mineral, Hyperspectral, atmospheric correction, multispectral, spectral signature.

1. Introduction

In recent times the use of mineral resources (base, precious or secondary metals, and rare earth elements), conventional hydrocarbon energy sources (oil, natural gas and coal), and obsolete hydrocarbons (oil shells) has increased rapidly. This has led to a higher demand for these resources and has resulted in a extensive need for improvement in natural resource exploration [1]. The development of mineral resources is an important factor in the planning and program of economic development of any country. In particular, in a situation of significant and growing scarcity, mineral resources are seen as a valuable resource of a country [2]. Heavy Minerals deposits in Bangladesh generally associated with sediments in paleobeach, paleovalleys and recent sandbars in rivers as well as recent beach area. Most of the paleobeach and shoreline of the world have a diverse range of economic minerals deposits such as rutile, zircon, ilmenite, garnet, magnetite, kyanite, leucoxene, and other heavy minerals. These minerals are principle source of important industrial minerals.

Heavy minerals are concentrated in back dune area of Cox's Bazar- Teknaf coast. Fore dune or the recent beach also contain noticeable amount of heavy minerals. Due to wave, current and wind actions, this part is very dynamic. The most significant metallic minerals are ilmenite, magnetite, rutile, zircon, garnet, monazite, kyanite, and leucoxene those are found on these sand deposits [3, 4].

For indirect exploration Remote Sensing is one of the utmost popular tools and is commonly used during the prospecting phase as it can provide a rapid assessment at a low cost and with minimal risk. This technique has been growing in line with technological advances in both its optical and radar applications. Optical sensors those are used in satellites have been effectively applied in geology to identify minerals and rocks, produce geological maps, and detect manifestations of mineral and hydrocarbon deposits and groundwater outflows by the reflectance and emissivity spectral characteristics of Earth surface materials [5, 6].

The study area was recognized earlier as one of the important placer deposits of heavy minerals. But unfortunately, the area became covered by different human activity within last two decades, such as household, agricultural activity, market, Rohingya rehabilitation camps, different government development activities, etc. Surficial heavy mineral almost disappeared in most of the area. The main objectives of present research are to identify the presence of heavy minerals through satellite image analysis and validation by field investigation.

2. Study Area

Part of Shilkhali and Lombori union of Teknaf upazilla under Cox's Bazar district (Figure 1) has been selected as study areas which were rich in heavy minerals as found in previous studies. The beach formation of Cox's Bazar-Teknaf area is a recent geological feature and has been formed on the wide and regionally extending gentle slope of the Shelf. Sediments deposited in these beach, are widely controlled by moderate ocean current dynamics. The black heavy mineral deposits, occurring as placer in the beach area, are mostly lenticular in shape. The deposits do exist both in the back dunes and in the fore dunes [7].

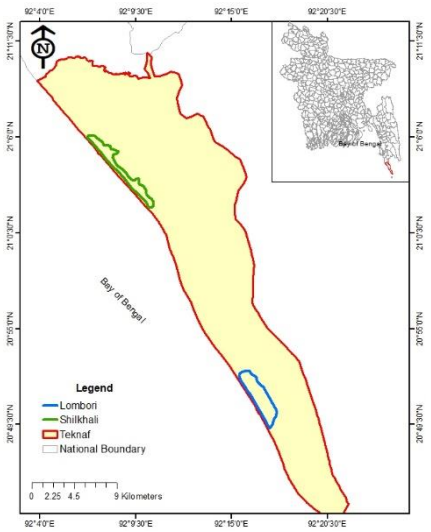

Figure 1: Location map of the study area

3. Methodology and Data Used

Figure 2 shows the methodological framework of the present research study. ENVI 6.4 version with the ArcGIS has been used for mapping heavy minerals from satellite imagery. For this purpose Landsat 8 OLI image of November 2020, January 2021, and April 2021 (Table 1) has been collected from the website https://earthexplorer.usgs.gov.

Table 1: List of data used in the Study

Satellite	Sensor	Path/Row	Acquisition Date	Resolution
Landsat 8	OLI	135/46	23 November 2020	30 M
			30 January 2021	
			04 April 2021	

First, the fast line-of-sight atmospheric analysis of spectral hypercubes (FLAASH) an atmospheric correction modeling tool is used to remove the atmospheric effects due to the presence of water vapor, aerosols, dust particles, etc. from satellite data. The reflectance calibration of the Landsat OLI data is performed with pre-launch gains and offsets calculated for Landsat sensors [8]. After obtaining suitable calibration parameters of the Landsat data, the model compensates for the atmospheric effects and retrieves the spectral reflectance from the multispectral radiance images. Finally, the preprocessed data is subjected to hourglass spectral analysis, which has the following steps [9, 10].

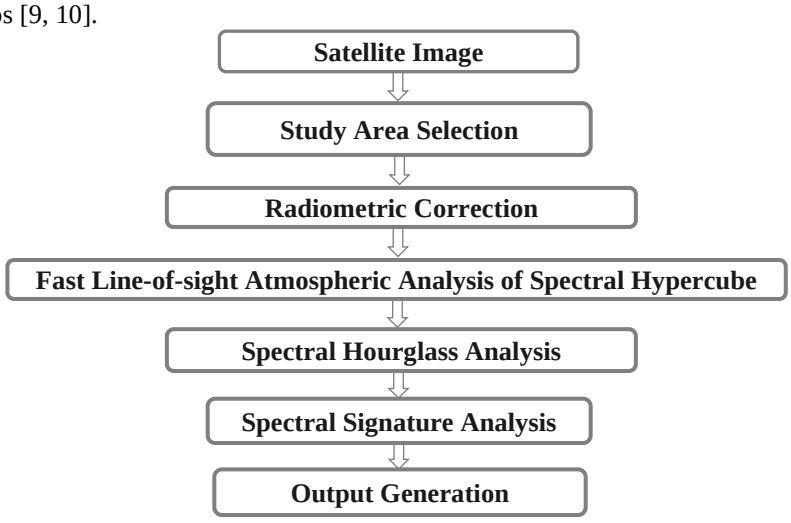

Figure 2: Flow Chart of the working methodology.

3.1 Minimum noise fraction transformation

To determine the inherent dimensionality of image data, to segregate noise in the data, and to reduce the computational requirements for subsequent processing ENVI's minimum noise fraction (MNF) transformation is used [11]. The advantages of MNF transformation over principal component analysis to reduce the dimensionality of hyperspectral imagery stated as Che-Ming Chen [12]. This transformation is applied to the atmospherically corrected and calibrated data and it generates seven MNF-transformed bands which can be viewed and analyzed.

3.2 Pixel purity index

To finding the most spectrally pure pixels in images ENVI's pixel purity index (PPI) is the best way [13,14]. By separating the most spectrally pure pixels it performs the spectral redundancy of data. The PPI reduces the number of pixels to be analysed in a data set and leads us to attain the spectrally unique target minerals or endmembers. The PPI generates an image in which pixel values correspond to the number of times that a pixel in the input data was recorded as extreme. This research work is carried out with the PPI analysis on the MNF bands with 1000 iterations and a threshold value of 3. The generated PPI image can be viewed and analyzed for locating the endmembers in an image.

3.3 n-Dimensional Visualizer

It is an interactive tool to locate, identify, and cluster the purest pixels and the most extreme spectral responses (endmembers) in a dataset in n-dimensional space. The generated pixel clouds can be rotated and visualized in different directions and angles. The visualizer helps to identify and isolate the target endmembers present in the data from the main clusters. The selected endmembers are verified by comparing and analyzing their spectral signatures with existing spectral reflectance data from USGS spectral libraries.

3.4 Mapping of minerals using spectral angle mapper

Spectral Angle Mapper (SAM) is a physically-based spectral classification that uses an *n*-D angle to match pixels to reference spectra. The algorithm determines the spectral similarity between two spectra by calculating the angle between the spectra and treating them as vectors in a space with dimensionality equal to the number of bands. This technique, when used on calibrated reflectance data, is relatively insensitive to illumination and albedo effects. Endmember spectra can be directly extracted directly from an image as region of interest (ROI) mean spectra. SAM compares the angle between the endmember spectrum vector and each pixel vector in *n*-D space. Smaller angles represent closer matches to the reference spectrum. Pixels further away than the specified maximum angle threshold in radians are not classified. USGS spectral library is used as reference spectrum.

4. Results & Discussion

The generated data space of the MNF transformation can be divided into two parts; one part is associated with large eigenvalues and coherent Eigen images. The other part is a complementary part with near-unity eigenvalues. Among the seven transformed MNF bands, the last two bands have the least information and are dominated by noise. They are omitted from further processing. Due to the application of the MNF transformation, the redundancy and noise in the data are eliminated and more-interpretable images are obtained. This operation was done for both study sites Shilkhali and Lombori of Teknaf.

Figure 3: Distribution of Heavy minerals in Shilkhali area reveal through spectral analysis of Landsat 8 OLI images of November 2020, January 2021and April 2021.

The PPI image (not shown) also helps to identify the target endmembers. The brighter pixels of the PPI-transformed image represent the most spectrally extreme pixels. To identify and locate the endmembers, the data clouds were visualized through the n-D Visualizer. In the visualizer, four separate clusters of pixels are seen in addition to the main cluster. The separate clusters may represent abundant mineral resources along the study area.

The spectral signatures of the obtained endmembers are very similar to the spectral signatures of rutile zircon, ilmenite, garnet, and augite. Finally, the endmembers are mapped with the SAM method. SAM is an automated

method for comparing image spectra to individual spectra or a spectral library [15]. It is also a per-pixel mapping method, which attempts to determine whether one or more target endmembers are abundant within each pixel in a hyperspectral (or multispectral) image based on the spectral similarity between the training (reference) pixel and target (unknown) spectra. The algorithm determines the similarity between two spectra by calculating the spectral angle between them, treating them as vectors in n-D space, where n is the number of bands. Smaller angles represent closer matches to the reference spectrum [10].

Figures 3, and 4 show the SAM-classified image representing the distribution of the heavy minerals along with the study areas. The classified images show that a large amount of augite with zircon, rutile, and garnet are deposited in the Shilkhali and Lombori study area. Ilmenite is also deposited in the Lombori area. Image analysis also reveals the seasonal impact on the presence of minerals.

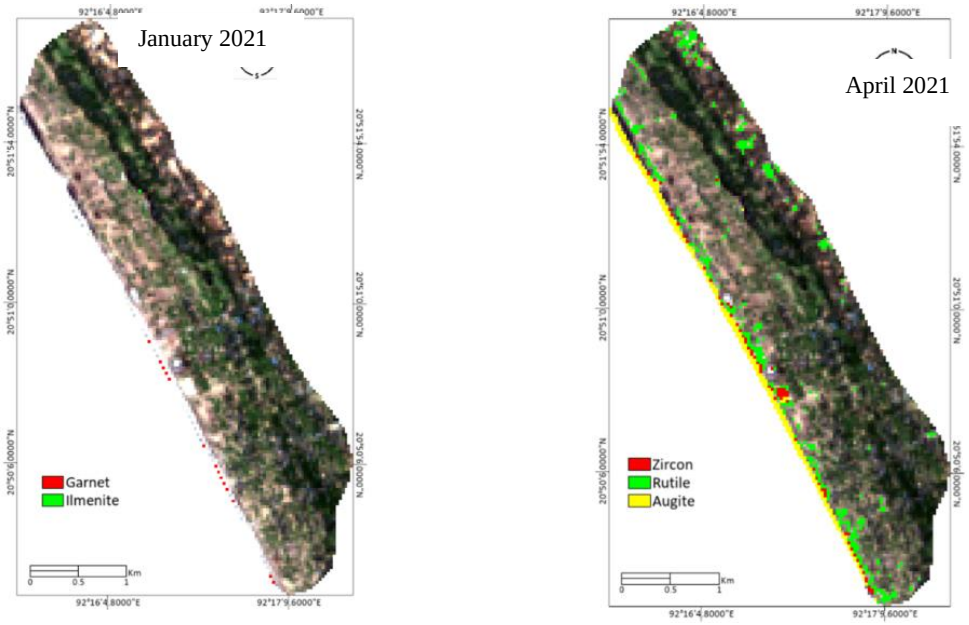

Figure 4: Distribution of Heavy minerals in Lombori, Teknaf area reveal through spectral analysis of Landsat 8 OLI image of January 2021 and April 2021.

4.1 Field Validation

Field verification of mineral resources has been performed to assess the accuracy of classification. The survey encompasses both the back dune and fore dune area along the coast of the study area. Total 38 surface samples were collected (18 samples from Shilkhali and 20 samples from Lombori) for further investigation in the laboratory. Sampling points were selected as a random pattern and the GPS coordinate of each sample was recorded.

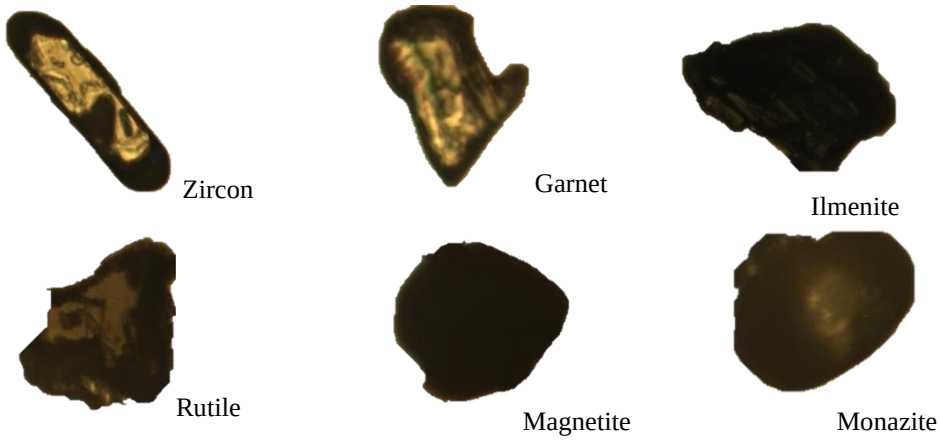

Figure 5: different heavy minerals identified during microscopic analysis.

Table 2: Individual Mineral percentage in raw sand (Shilkhali, Teknaf)

Sample ID	Total Heavy mineral %	Opaque (Ilmenite+ Magnetite)	Garnet	Zircon	Rutile	Monazite	Others
SL 1	3.93	1.56	0.46	0.07	0.03	0.01	1.81
SL 2	34.53	9.68	3.07	2.95	0.11	0.42	18.29
SL 3	12.79	3.79	1.25	0.49	0.06	0.06	7.14
SL 4	4.71	1.17	0.72	0.10	0.02	0.01	2.69
SL 5	25.80	6.13	4.17	0.67	0.11	0.20	14.52
SL 6	46.01	16.88	4.08	2.31	0.16	0.19	22.39
SL 7	30.33	9.50	2.87	2.18	0.14	0.23	15.41
SL 8	33.59	11.97	3.39	2.28	0.17	0.13	15.65
SL 9	18.09	6.00	1.70	0.94	0.09	0.12	9.23
SL 10	11.72	3.91	1.21	0.35	0.06	0.05	6.15
SL 11	18.64	4.99	2.49	1.24	0.09	0.21	9.63
SL 12	26.92	9.87	2.82	1.45	0.16	0.13	12.50
SL 13	12.80	3.53	1.59	1.09	0.07	0.17	6.35
SL 14	18.53	5.96	4.36	0.43	0.11	0.08	7.58
SL 15	18.71	5.68	1.91	0.60	0.10	0.16	10.27
SL 16	14.21	3.88	1.93	0.30	0.07	0.09	7.94
SL 17	5.22	1.43	0.72	0.12	0.01	0.01	2.94
SL 18	5.07	1.21	0.65	0.25	0.03	0.04	2.88

Table 3: Individual Mineral percentage in raw sand (Lombori, Teknaf).

Sample ID	Total Heavy mineral %	Opaque (Ilmenite+ Magnetite)	Garnet	Zircon	Rutile	Monazite	Others
TK 1	22.25	6.72	2.94	1.11	0.09	0.06	11.32
TK 2	80.59	31.44	10.91	6.61	0.73	0.36	30.54
TK 3	6.21	2.19	1.12	0.30	0.08	0.04	2.49
TK 4	15.71	6.04	3.26	0.48	0.16	0.08	5.70
TK 5	35.16	9.09	9.09	1.16	0.18	0.14	15.51
TK 6	14.59	5.60	2.99	0.37	0.13	0.07	5.43
TK 7	18.13	6.76	3.43	0.65	0.10	0.03	7.16
TK 8	9.90	3.40	1.64	0.64	0.12	0.10	4.00
TK 9	29.49	9.94	4.14	1.50	0.13	0.17	13.62
TK 10	8.60	3.09	0.94	0.26	0.04	0.03	4.24
TK 11	9.71	3.01	1.23	0.44	0.05	0.03	4.94
TK 12	15.00	5.45	2.45	0.74	0.08	0.02	6.25
TK 13	4.45	1.35	0.85	0.21	0.02	0.02	2.00
TK 14	3.65	1.43	0.57	0.21	0.02	0.02	1.40
TK 15	3.76	1.25	0.79	0.44	0.04	0.03	1.90
TK 16	20.01	7.47	4.00	1.21	0.16	0.12	7.04
TK 17	15.86	5.37	2.05	0.53	0.09	0.08	7.74
TK 18	76.21	23.62	12.08	10.72	0.48	0.73	28.58
TK 19	21.47	6.36	4.42	1.16	0.30	0.19	9.03
TK 20	8.20	2.96	1.94	0.50	0.17	0.06	2.57

Each sample was undergone oven-dry until all of the moisture was released. Dry samples were passed through the elimination process of unwanted material like a tree root, marine organism shell, etc. Then, samples were washed with fresh water using a sieve mesh size of 55µm ensuring any sand grain is not removed by water. All samples were subjected to bromoform separation ($CHBr_3$ with specific gravity 2.89). Separated heavy minerals were investigated under an optical polarized microscope (Optima ML9000) by applying the grain counting technique (Figure 5). Temporary slides were prepared for this analysis to identify individual minerals based on their optical properties. According to the standard procedure, mineral grains were counted from 10 views for each slide (i.e. samples) with at least 100 grains in each view, which leaves a total minimum of 1000 grains for each sample. Adjusting with the specific gravity, the concentration of identified minerals was calculated as weight percentage (Table 2 and 3).

The accuracy of image classification and the mapping of mineral deposits can be assessed by comparing the heavy mineral contents of the sediment sample and the type of classified pixel corresponding to the location of the sample.

From laboratory analysis, it is seen that average quantity of heavy minerals in Shilkhali area is 18.987% and Lombori area is 20.947 %. At Shilkhali, maximum abundance of heavy minerals (46.01%) was found in sample no SL-6 and at Lombori, maximum abundance of heavy minerals (80.59%) was found in sample no TK-2. All the samples were collected from surface of the deposits where heavy minerals concentration is generally low. Heavy minerals concentration is relatively greater in subsurface (up to 5 ft depth). In mineralogical point of view, the area is dominated by garnet, ilmenite & magnetite with considerable amount of zircon, rutile, monazite and also presence of some other unidentified heavy minerals.

Presence of heavy minerals on surface of the deposits is not prominent due to human activity and vegetation cover. However, subsurface condition of heavy minerals may remain unchanged compared to previously identify heavy minerals deposits along back dune area. But fore dune area, i.e. near shore line is variable because it experiences successive erosion and deposition and this area is directly attached with Ocean current dynamics of the Bay of Bengal.

5. Conclusion and Recommendation

Remote sensing is a useful tool in mapping the mineral resources along with coastal areas. In this study, the potential use of multispectral Landsat data for mapping heavy-mineral resources has been demonstrated. The minerals which show significant variation in reflectance at different spectral bands can be effectively mapped by using multispectral data. The classified image shows that a large amount of augite is deposited along the shoreline of the study area. Ilmenite garnet, rutile, and zircon are also deposited along the coast. It is very helpful to identify and locate the abundance of minerals, which leads to the eco-friendly and sustainable exploitation of minerals resources along the study area. It also emphasizes the ability and application of Landsat data to investigate potential mineral resources. Field validation supports the presence of ilmenite garnet, rutile, and zircon but augite in the study area. It is also clear that the identification of minerals from satellite image is time sensitive. Presence of these mineral may vary time to time due to moisture condition, vegetation cover and atmospheric effects. Multispectral satellite images have limitations because of their low band numbers. Hyperspectral images have special advantages in mineralogical applications. For more accurate results hyperspectral imagery has to be used. To minimize the effect of mixed pixels and extract better information use of high spatial resolution image is highly recommended for future work. Collection of spectral signature from the field using spectro-radiometer will enhance the accuracy of the research.

Acknowledgements

The author is thankful to Beach Sand Mineral Exploitation Center (BSMEC), Cox's Bazar of Bangladesh Atomic Energy Commission (BAEC) for working as a collaborative partner in this research work.

References

[1] Hede, A., N., H., 2016. Development and Application of Geobotanical Remote Sensing Methods for Mineral Exploration in Thick Vegetation Areas, Ph. D Dissertation (Unpublished), Graduate School of Engineering, Kyoto University.

[2] Faruque, A. A., 2018. Bangladesh: Legal Framework on Mineral Exploration, Springer-Verlag GmbH Germany, part of Springer Nature 2018, G. Tiess et al. (eds.), Encyclopedia of Mineral and Energy

[3] Kabir, M.Z., Deeba, F., Rasul, M.G., Majumder, R.K., Khalil, M.I. and Islam, M.S., 2018. Heavy Mineral Distribution and Geochemical Studies of Coastal Sedimentsat Sonadia Island, Bangladesh, Journal of Nuclear Science. Policy, https://doi.org/10.1007/978-3-642-40871-7_151-1.

[4] Deeba, F., Kabir, M.Z., Zaman, M.M., Rajib, M. and Rana, S.M., 2009. Difference in Grain Size Distribution Among Heavy Minerals of Cox's Bazar, Barchara, Patuartek and Teknaf Fore Dune Deposit, Proceed. of Int. Confer. on Geosci. for Glob. Dev., 26-31 October, 2009, Dhaka, Bangladesh, 24-27.

[5] Koide, K., & Koike, K. (2012). Applying vegetation indices to detect high water table zones in humid warm-temperate regions using satellite remote sensing. International Journal of Applied Earth Observation and Geoinformation, 19, 88–103. http://doi.org/10.1016/j.jag.2012.03.017

[6] Sabins, F. F., 1999. Remote sensing for mineral exploration. Ore Geology Reviews, 14(3-4),157–183. http://doi.org/10.1016/S0169-1368 (99)00007-4

[7] Chowdhury, M.I. and Sarker, M.N., 2014. Delineation of the Surface Pattern of Heavy Mineral Deposit of Tulatoli Paleo Dune Within Teknaf Beach Strip of Cox's Bazar District with Radiometric Survey. Nuclear science and applications, Vol. 2 3. No. 1&2.

[8] MARKHAM, B.L. and BARKER, J.L., 1986, Landsat MSS and TM post-calibration dynamic ranges, exoatmospheric reflectances and at-satellite temperatures. EOSAT Landsat technical notes, pp. 3–8.

[9] Gazi, M. Y., Tafhim, K. T., Ahmed, M. K. and Islam, M. A., 2019. Investigation of Heavy-Mineral Deposits Using Multispectral Satellite Imagery in the Eastern Coastal Margin of Bangladesh, Journal of Earth Sciences Malaysia (ESMY), ISSN: 2521-5043 (online)

[10] Chandrasekar, N., Sheik Mujabar, P. & Rajamanickam G.V., 2011. Investigation of heavy-mineral deposits using multispectral satellite data, International Journal of Remote Sensing, 32:23, 8641-8655, DOI: 10.1080/01431161.2010.545448

[11] Boardman, J.W. and KRUSE, F.A., 1994. Automated spectral analysis: a geologic example using AVIRIS data, north Grapevine Mountains, Nevada. In Proceedings of Tenth Thematic Conference on Geologic Remote Sensing, 9–12 May 1994, San Antonio, TX (Ann Arbor MI: Environmental Research Institute of Michigan), pp. I-407–I-418

[12] Che, Ming Chen., 2000. Comparison of principal components analysis and minimum noise fraction transformation for reducing the dimensionality of hyperspectral imagery. Geographical Research, 33, pp. 163–178.

[13] Boardman, J.W., 1993. Automating spectral unmixing of AVIRIS data using convex geometry concepts. In 4th JPL Airborne Geoscience Workshop, Washington, DC (Pasadena, CA: Jet Propulsion Laboratory), pp. 11–14.

[14] Boardman, J.W., Kruse, F.A. and green, R.O., 1995. Mapping target signatures via partial unmixing of AVIRIS data. In Summaries of the 5th Annual JPL Airborne Geoscience Workshop, 23–26 January 1995, Pasadena, CA (Pasadena: Jet Propulsion Laboratory), pp. 23–26.

[15] Boardman, J.W. and HUNTINGTON, J.F., 1996. Mineral mapping with 1995 AVIRIS data. In Summaries of the Sixth Annual JPL Airborne Research Science Workshop (JPL Publication 96-4), vol. 1, pp. 9–11 (Pasadena, CA: Jet Propulsion Laboratory).